

MM2 Calculations on Cyclodextrins: Multimodal Inclusion Complexes

F. Pérez,[†] C. Jaime,* and X. Sánchez-Ruiz

Departament de Química, Facultat de Ciències, Universitat Autònoma de Barcelona,
08193 Bellaterra, Barcelona, Spain

Received July 14, 1994[®]

The properties of cyclodextrin multimodal inclusion complexes were correctly reproduced by MM2-(85) calculations. In spite of the two largest inherent limitations (use of a model and absence of solvent), the method used allows for the correct determination of the complex geometry not only within totally different molecules but also when the differences in the complexes are subtle as a consequence of being produced by the complexation of enantiomeric forms.

Introduction

The ability of β -CD to form inclusion complexes with different products^{1–6} is well-known. It has been used in stabilizing light-sensitive compounds, in modifying the physical and chemical properties of guests (solubility, volatility, flavor, and taste), and as drug carriers. The fact that β -CD or some derivatives present enzymatic activity is especially interesting due to the similarity with enzyme–substrate interactions. The basis of these phenomena is the ability to recognize and include molecules. The study of β -CD inclusion complexes may be of great interest for the synthetic development of artificial enzymes,⁷ molecular recognition, and supramolecular chemistry.⁸ The β -CD molecule is built up from seven glucopyranose units with $\alpha(1,4)$ glycosidic type bonds adopting a torus shape and leaving a hydrophobic cavity able to include a wide range of organic molecules. To study inclusion complexes and their geometry, several methods have been used: thermogravimetry, differential scanning calorimetry, IR spectroscopy, UV spectroscopy, fluorescence spectrophotometry, circular dichroism, nuclear magnetic resonance (NMR), X-ray diffraction, neutron diffraction, electron paramagnetic resonance (EPR), electron double resonance (ENDOR), and theoretical calculations.

Since β -CD has a chiral structure, both enantiomers from the same guest will form diastereomeric complexes. It may be assumed that each has a different geometry to achieve the best host–guest fit. In fact, a nonrigid guest may not keep the same conformation when complexed as when it is alone, and it can even show another geometry in a complex at which it has a lower total energy. The study of inclusion processes in such cases becomes difficult. The dynamic situation means that techniques with long acquisition times present average

situations of the whole process. For example, in the case of a quick formation–dissociation equilibrium among different complexes in solution, it is difficult to detect them exclusively by NMR techniques. On the other hand, different complexes can be detected by the EPR–ENDOR technique (with a shorter time scale) using a paramagnetic guest (e.g., nitroxide radical). The combination of experimental and computational methods can be a good tool for determining the complex geometry.

Recently, the complexation of different substrates in racemic form (**1**, **2**, **3**, and **4**) has been studied by EPR–ENDOR techniques.⁹ Each product has an asymmetric carbon, and owing to the exclusive D-glucopyranose constitution of β -CD, six diastereomeric complexes are possible. Kotake and Jansen found three complexes for guests **1** and **4** (one for each group-in) and four complexes for **2** and **3** (with more than one diastereomeric complex in each case). Due to the similarity between the signals, only complexes with the *tert*-butyl group-in were assigned. As a result of the dependence between $\alpha_{\beta-H}$ and the square of the cosine of the H–C–N–O dihedral angle, an attempt has been made to model the complexation process between these nitroxides and β -CD. The process was studied by molecular mechanics using Allinger's MM2(85)¹⁰ force field, modified so as to include the hydrogen bond treatment.¹¹ This force field was chosen because of the good correlation between experimental data and geometries^{12–17} calculated using this force field.

Computational Method

Host. The β -CD coordinates were taken from the published neutron diffraction structure¹⁸ and were re-

[†] On a leave of absence from Laboratori de Química Farmacèutica, Facultat de Farmàcia, Universitat de Barcelona, Av. Diagonal s/n, 08028 Barcelona, Spain.

[®] Abstract published in *Advance ACS Abstracts*, May 15, 1995.

(1) Szejtli, J. *Cyclodextrins and their Inclusion Complexes*; Akadémiai Kiadó: Budapest, 1982.

(2) Szejtli, J. *Cyclodextrin Technology*; Kluwer Academic Publishers: Dordrecht, 1988.

(3) Saenger, W. *Angew. Chem., Int. Ed. Engl.* **1980**, *19*, 344.

(4) Duchêne, D., Ed. *New Trends in Cyclodextrins and Derivatives*; Editions de Santé: France, 1993.

(5) Schneider, H. *Angew. Chem., Int. Ed. Engl.* **1991**, *30*, 1417.

(6) Atwood, J. L.; Davies, J. E. D.; MacNicol, D. D., Eds. *Inclusion Compounds*; Academic Press: London, 1984; Vols. 1–3.

(7) Sasaki, S.; Takase, Y.; Koga, K. *Tetrahedron Lett.* **1990**, *31*, 6051.

(8) Vogtle, F. *Supramolecular Chemistry: an Introduction*; John Wiley & Sons: New York, 1991.

(9) Kotake, Y.; Janzen, E. G. *J. Am. Chem. Soc.* **1992**, *114*, 2872.

(10) Allinger, N. L. Available from QCPE or from Molecular Design Ltd., 2132 Farallon Dr., San Leandro, CA 94577 (PC version by A. Buda).

(11) Allinger, N. L.; Kok, R. A.; Imam, M. R. *J. Comput. Chem.* **1988**, *9*, 591.

(12) Fathallah, M.; Fotiadu, F.; Jaime, C. *J. Org. Chem.* **1994**, *59*, 1288.

(13) Fotiadu, F.; Fathallah, M.; Jaime, C. *J. Inclusion Phenom.* **1993**, *16*, 55.

(14) Lipkowitz, K. B.; Raghothama, S.; Yang, J. *J. Am. Chem. Soc.* **1992**, *114*, 1554.

(15) Jaime, C.; Redondo, J.; Sánchez-Ferrando, F.; Virgili, A. *J. Mol. Struct.* **1991**, *248*, 317.

(16) Redondo, J.; Jaime, C.; Virgili, A.; Sánchez-Ferrando, F. *J. Org. Chem.* **1990**, *55*, 4772.

(17) Linert, W.; Han, L.; Lukovits, I. *Chem. Phys.* **1989**, *139*, 441.

(18) Betzel, C.; Saenger, W.; Hingerty, B. E.; Brown, G. M. *J. Am. Chem. Soc.* **1984**, *106*, 7545.

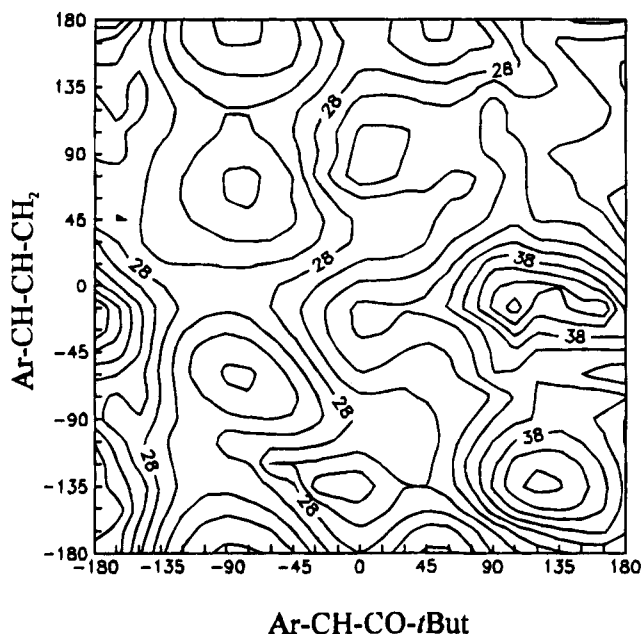


Figure 1. Theoretical conformational map for the variation of Ar-CH-CO-*t*-Bu and Ar-CH-CH-CH₂ dihedral angles of **7** by the MM2(85) force field.

fined for our calculations (undetermined hydrogen atoms and all the lone pairs were added).¹⁶ Allinger's MM2-(85)¹⁰ force field was used. The β -CD molecule was oriented with all the glycosidic oxygen atoms in the XY plane, the Z-axis in the geometric center of the heptagon formed by the oxygens, and the wider half of the β -CD torus placed in the negative zone of the Z-axis.

Guest. As the N-O bond has no parameters in the MM2 force field, it was replaced by a C=O bond because of their similar geometries.¹⁹ This replacement generates products **5–8** which were used in our calculations as models for compounds **1–4**.

	$\begin{array}{c} R_1 \\ \diagup \\ N^+-tBu \\ \diagdown \\ R_2 \end{array}$	$\begin{array}{c} R_1 \\ \diagup \\ C=O-tBu \\ \diagdown \\ R_2 \end{array}$	
	R ₁	R ₂	
1	Ph	CH ₃ -O-Ph	5
2	Ph	CH ₃ -Ph	6
3	C ₆ H ₁₁	CH ₃ -O-Ph	7
4	<i>n</i> -Hex	Ph	8
11	Ph	Ph	

For all isolated guests, a full conformational study was carried out by rotating the Ar-C1 bond from 0 to 180° and the CO-C1 bond from -180 to 180° in 10° steps using the two-bond drive technique (Figure 1 shows the contour map corresponding to the energy surface of **7** as an example). For compound **7**, only the envelope conformations were considered, and in compound **8**, the *n*-hexyl chain was considered *all-anti*. For **8**, the C1-*n*-hexyl bond was rotated to obtain two isoenergetic minima having bonds Ph-*n*-Hex and *t*-Bu-*n*-Hex in *anti* conformations. The energy minima obtained were fully optimized without restrictions. The most stable conformation¹² of **5**, **6**, and **7** and the two conformers of **8** were used in our calculations.

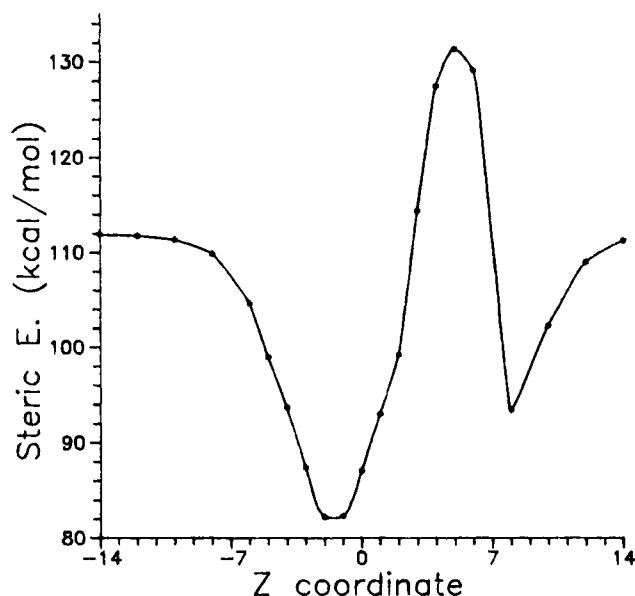


Figure 2. Total steric energy variation for the simulation of the β -CD complexation of **5** in the *tert*-butyl-in orientation.

Orientations. Six orientations of each product were considered (one for each group attached on C1 of the *R* and *S* enantiomer). For each group attached, two atoms were kept on the Z-axis to simulate the possible complex: (1) C of carbonyl and quaternary C of *tert*-butyl, (2) C1 and C_{ipso} for rings, and (3) C1 and the second C of the *n*-hexyl chain for **8**.

Inclusion Process. A published method was followed:¹³ The guests were located, in proper orientation, at a Z-coordinate of -14 Å and were moved through the host cavity along the Z-axis to +14 Å in 2 Å steps (from -14 to -6 Å and from +6 to +14 Å) or in 1 Å steps (from -6 to +6 Å). The first atom of the oriented group attached to C1 was the reference Z-coordinate, and its movement was totally restricted. Since the β -CD has an almost heptagonal symmetry, the guests were rotated 51.4° (360°/7) in 10.3° steps from an arbitrary starting position. The systematic variation of translation and rotation along the Z-axis produces an energy surface. The different minima found on it were minimized again without restrictions for the guest.

Results and Discussion

Complexation Process. The translation of a guest through the β -CD molecule (-14 to +14 Å) (Figure 2) shows two minima separated by a high-energy barrier, with the sole exception being molecule **8**, for which the *tert*-butyl-in complex presents a small barrier because the *n*-hexyl chain changes its conformation to reduce interactions (the second dihedral angle changes from about 180° to almost 60°). Figure 2 contains the graph of the energy variation for compound **5** in the *tert*-butyl-in orientation as an example.

The lowest energy minimum is obtained when one of the C1 substituents resides within the β -CD cavity while other groups remain outside in the wider edge of β -CD. This geometry corresponds to the inclusion complex. The greatest internal diameter of β -CD is around 6.2 Å, and the volume of the guests is too large to be totally included. However, we have modeled the inclusion process by a translation of a whole guest through the host by entering *via* the wider end. Nonreal high-energy barriers were

(19) Roberts J. S. *Comprehensive Organic Chemistry*; Pergamon Press: Oxford, 1979; Vol. 2, p 279.

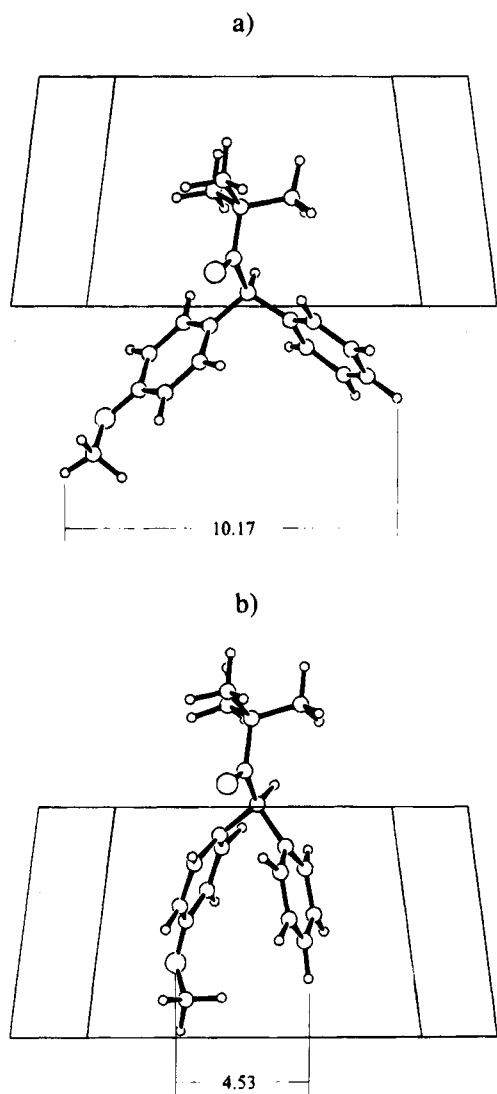


Figure 3. 3. ORTEP²⁰ diagrams of the guest and schematic representations of β -CD for clarity (with distance in angstroms between more external atoms of guest) in the complexation process of S-5 (a) at -2 Å of Z-coordinate and (b) at $+5$ Å of Z-coordinate.

obtained when the guest resided within the β -CD cavity due to strong repulsive interactions and to the increase in bending and torsion energy. The other energy minimum observed in Figure 2 has a geometry such that the guest is totally outside the β -CD cavity at the upper edge and the host-guest interactions are thus very small. Figure 3 shows the ORTEP²⁰ drawing of the isolated guest in the complexation process of S-5 in the *tert*-butyl orientation at -2 and $+5$ Å of the Z-coordinate. Note that the distances between the outermost atoms are 10.17 and 4.53 Å, respectively. For each compound, only one full inclusion was calculated (from -14 to $+14$ Å Z-coordinates) to reduce the CPU time required. Other translations (for different rotational starting points) were calculated from -14 to $+4$ Å Z-coordinates.

The combination of translation and rotation of the guest along the Z-axis produces an energy surface. Figure 4 shows the energy surface obtained for the inclusion of S-7 in the cyclopentyl-in orientation as an example.

The guest was rotated 51.4° in steps of 10.3° , owing to the pseudo-C₇ symmetry of β -CD and the asymmetry of the whole guest, and although more than one energy minimum is possible, only one or two minima were obtained on the energy surface of each inclusion process modeled, probably due to nonbonding interactions between atoms. Two of the guest atoms are fixed in our method, one in the Z-coordinate to simulate the translation movement and the other in the XY-plane to simulate the rotation. All the minima and the nearest points (within a range of $+7$ kcal/mol) were minimized again without the restrictions corresponding to the guest because small differences in the initial energy may give rise to large changes in the final energy (and geometry) due to hydrogen bond formation between some of the host hydroxyls and one of the guest methoxy groups.

The final geometry was obtained by averaging the measures using Boltzman's equation to calculate the conformer population for each inclusion complex (all conformers having more than 1% of the population were considered). Only five conformers (phenyl-in type) were neglected because they showed a hydrogen bond between one primary hydroxyl in the upper surface of β -CD and the phenyl ring. Probably, the primary hydroxy groups may form hydrogen bonds with the solvent, as water is present in large quantities and forms much stronger hydrogen bonds with hydroxyl groups than with phenyl groups.^{11,21}

Two other types of hydrogen bonds involving the oxygen of a methoxyl group or the oxygen of the carbonyl group were detected. Both types of hydrogen bonds are always formed with the primary or secondary alcohols. When the molecule has a methoxy group, a hydrogen bond between this group and one β -CD hydroxy group was found. The carbonyl group forms hydrogen bonds in most of the conformers where the *tert*-butyl is not included, except for the *tert*-butyl-in complex of molecule 8, in which the carbonyl presents hydrogen bonds with the primary hydroxyls. This last type of hydrogen bond deserves special consideration because the nitroxide radical of the original molecules has been replaced by a carbonyl group, owing to their geometrical similarity. Although formation of hydrogen bonds between hydroxy groups and nitroxide radicals has been described,²² the trend of formation and bond strength can be very different from that of a carbonyl group. Although it is not the aim of this study to reproduce the energy of complexation, but rather to determine the geometry of the complex, we decided to validate the nitroxide-carbonyl substitution by semiempirical calculations (AM1) using 4-hydroxybutan-2-one as a pattern. The conformational map was made by deriving the $\text{CH}_2\text{-O}$ (w_1) and $\text{CH}_2\text{-CH}_2$ (w_2) bonds; then we rotated the C(O)-CH_2 (w_3) bond for each minimum found. Finally, all minima were minimized again without restrictions. Five minima were found: three local minima at approximately (w_1, w_2, w_3) = (180, 180, 180), ($\pm 60, 180, 180$) and two absolute minima at ($-60, 60, 180$) and ($60, -60, 180$). These last minima show intramolecular hydrogen bonds. *Ab initio* calcula-

(20) Johnson, C. K. ORTEP-II. Report ORNL-5138; Oak Ridge National Laboratory: Oak Ridge, TN, 1976.

(21) Biali, E. S.; Rappoport, Z. *J. Am. Chem. Soc.* **1984**, *106*, 5641.

(22) Haire, D.; Kotake, Y.; Janzen, E. G. *Can. J. Chem.* **1988**, *66*, 1901.

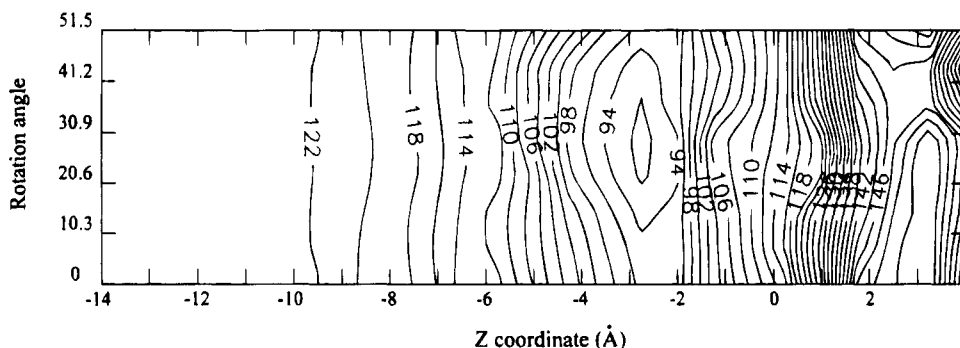


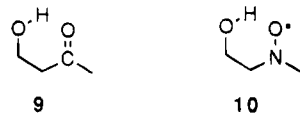
Figure 4. Contour map representation of the energy surface for the inclusion of S-7 in the cyclopentyl-in orientation.

Table 1. Significant Data for the Conformers of Compounds 9 and 10 by AM1 and *ab Initio* (MP2) Calculations

compd	ω_1^a	ω_2^b	ω_3^c	ΔH_f^d	$\Delta \Delta H_f^d$	ΔE_{MP2}^e
9a	180.02	179.98	180.01	-100.61	2.46	4.01
9b ^f	65.40	178.13	-179.12	-101.68	1.39	4.09
9c ^f	-68.11	65.12	174.89	-103.07	0.00	0.00
10a	175.68	-177.94	-173.97	-48.90	4.06	7.07
10b ^f	-70.46	-179.61	-175.39	-50.18	2.78	6.67
10c ^f	-68.41	72.25	177.22	-52.96	0.00	0.00

^{a-c} Dihedrals CH₂-CH₂-O-H, C-CH₂-CH₂-O, and CH₃-C-CH₂-CH₂, respectively, in degrees. ^d Kilocalories per mole by AM1. ^e Kilocalories per mole by *ab initio* (MP2). ^f There is an enantiomeric conformer.

tions (MP2 3-21G) with Gaussian 92 program²³ were also carried out to reinforce the validity of the AM1 calculations. Structures 9b and 10b were initially fully optimized. Analyses of the influence of each structural



parameter set (bond lengths, bond angles, and dihedral angles) on the final energy demonstrated that bond lengths were the parameters introducing larger energy changes. Starting geometries of each conformer were built taking bond and dihedral angles from AM1 calculations and bond lengths from MP2 calculations. Final geometries were obtained by a process in which only bond lengths and angles around N-O (or C=O) and O-H groups were allowed to be optimized. For each compound, the conformer having a H bond is shown to have the lowest energy. Both MO calculations indicate that substitution of carbonyl groups by nitroxide radicals produces similar geometries but larger energy differences (see Table 1), favoring the H bond in the nitroxide derivatives.

Hydrogen bonds have been formed because of the natural proximity of the groups due to the size of the two molecules, without leading to great conformational changes either in β -CD or in the guest. Perhaps the most important factor to consider is the solvent. Due to the method requirements, all calculations refer to the gas phase and, therefore, energies obtained must be related with enthalpies. From the agreement between the experimental and calculated data, we have assumed that

the solvent always has the same effect (the reason is that all molecules compared are similar in structure and are strongly hydrophobic). An interesting discussion can be found in ref 12.

Guest Geometry and EPR Measurements. Two types of hyperfine splitting constants (hfsc) are available from the nitroxides 1-4 due to nitrogen and hydrogen atoms. It is known^{24,25} that the probe's nitrogen hfsc (a_N) decreases in the complex compared to the free probe in water due to the more hydrophobic environment. These different nitrogen hfsc (a_N) allowed Kotake and Janzen to assign⁹ the *tert*-butyl-in complex for each probe. Obviously, the a_N changes its value only when the host and guest interact (*i.e.*, at short distances). When the molecules are far apart, no detectable change on the guest a_N value, depending on the host-guest distance, will be observed, as a direct consequence of having a similar hydrophobic guest environment. Table 2 contains the experimental a_N values for all the nitroxide compounds (1-4) and the calculated distance from the carbonyl O (equivalent to the nitroxide O) to the plane defined by all the β -CD glycosidic oxygens within a particular complex. If we take this distance as a measure of the degree of inclusion (more inclusion means more hydrophobic environment), an acceptable correlation ($0.75 < r < 0.93$) is obtained between this distance and the experimental a_N values. A similar correlation is obtained ($0.70 < r < 0.99$) when representing a_N against the inverse of the calculated distance. The calculated distance for the *tert*-butyl-in of S-8 seems to be too different from that R-8 (Table 2). The inadequacy of the Block-diagonal algorithm in minimizing structures with a large number of atoms may be the reason for this discrepancy. When the point corresponding to the S-8 *tert*-butyl-in complex is removed, better correlation coefficients are obtained ($0.91 < r < 0.99$).

On the other hand, $a_{\beta-H}$ depends on the dihedral angle between the nitrogen p-orbital and the C-H bond (θ) and on the nitrogen spin density (ρ_N), as expressed by the Heller-McConnell equation:²⁶ $a_{\beta-H} = (A + B \cos^2 \theta) \rho_N$. Other factors are the bulkiness and the electronegativity of attached groups on nitrogen.²⁷⁻²⁹ More bulky groups increase the β -hfsc; otherwise, more electronegative groups decrease the β -hfsc. Table 3 shows the H-C-

(24) (a) Kotake, Y.; Janzen, E. G. *J. Am. Chem. Soc.* **1988**, *110*, 3699. (b) Janzen, E. G.; Coulter, G. A.; Oehler, U. M.; Bergsma, J. P. *Can. J. Chem.* **1982**, *60*, 2725.

(25) Reddoch, A. H.; Konishi, S. *J. Chem. Phys.* **1979**, *70*, 2121.

(26) Heller, C.; McConnell, H. M. *J. Chem. Phys.* **1960**, *32*, 1535.

(27) Kotake, Y.; Janzen, E. G. *J. Am. Chem. Soc.* **1989**, *111*, 5138.

(28) Terabe, S.; Konaka, R. *J. Chem. Soc., Perkin Trans. 2*, **1972**, 2163.

(29) Terabe, S.; Konaka, R. *J. Chem. Soc., Perkin Trans. 1*, **1973**, 369.

(23) Frisch, M. J.; Trucks, G. W.; Head-Gordon, M.; Gill, P. M. W.; Wong, M. W.; Foresman, J. B.; Johnson, B. G.; Schegel, H. B.; Robb, M. A.; Replogle, E. S.; Gomperts, R.; Andres, J. L.; Raghavachari, K.; Binkley, J. S.; Gonzalez, C.; Martin, R. L.; Fox, D. J.; Defrees, D. J.; Baker, J.; Stewart, J. J. P.; Pople, J. A., *Gaussian 92*, Revision C; Gaussian Inc.: Pittsburgh, PA, 1992.

Table 2. Experimental^a a_N Values and Calculated Distances from the Carbonylic Oxygen to the Plane Defined by All the β -CD Glycosidic Oxygens

	a_N			distance ^a (1/distance)		corr coeff
	free	<i>t</i> -Bu-in	others-in	<i>t</i> -Bu-in	others-in	
<i>R</i> -5	1.59 ^b	1.54 ^b	1.60 ^b , 1.60 ^b	0.79 (1.27)	1.48 ^f (0.676), 2.65 ^g (0.377)	0.75 (0.91)
<i>S</i> -5				0.61 (1.64)	1.22 ^f (0.820), 2.66 ^g (0.376)	
<i>R</i> -6	1.59 ^c	1.57 ^c	1.60, ^c 1.60, ^c 1.60 ^c	0.57 (1.75)	2.73 ^h (0.366), 2.07 ^g (0.483)	0.97 (0.99)
<i>S</i> -6				0.51 (1.96)	2.44 ^h (0.410), 2.20 ^g (0.455)	
<i>R</i> -7	1.60 ^d	1.58 ^d	1.60, ^d 1.60, ^d 1.60 ^d	1.62 (0.617)	3.05 ⁱ (0.328), 3.41 ^g (0.293)	0.86 (0.91)
<i>S</i> -7				1.95 (0.512)	2.40 ⁱ (0.417), 2.81 ^g (0.356)	
<i>R</i> -8	1.58 ^e	1.57 ^e	1.58, ^e 1.58 ^e	1.11 (0.901)	2.43 ^f (0.412), 2.99 ^g (0.334)	0.93 ^k (0.70)
<i>S</i> -8				0.18 (5.56)	2.55 ^f (0.392), 2.21 ^j (0.452)	

^a In angstroms. ^{b-e} Values refer to nitroxides 1–4, respectively. ^f Phenyl-in. ^g Anisyl-in. ^h Tollyl-in. ⁱ Cyclopentyl-in. ^j *n*-Hexyl-in. ^k 0.91 (0.98) if *S*-8 *tert*-butyl-in is removed.

Table 3. Experimental^a $a_{\beta-H}$ Values, Calculated Dihedral Angles H–C–C=O (in degrees), and Best Correlation Coefficients Obtained from the Multilinear Regression Analysis

compd	experimental $a_{\beta-H}$ ⁹			calculated H–C–C=O			<i>r</i>
	free	<i>t</i> -Bu-in	others-in	free	<i>t</i> -Bu-in	others-in	
<i>R</i> -5				150.5	149.6	134.4, ^a 151.2 ^b	0.99
1	0.43	0.442	0.313, 0.285				
<i>S</i> -5				145.5	131.5 ^a	158.6 ^b	0.99
<i>R</i> -6				148.9	148.5	160.5, ^c 137.6 ^b	
2	0.43	0.441	0.364, 0.313, 0.280				0.97
<i>S</i> -6				134.8	152.3 ^c	138.3 ^b	
<i>R</i> -7				145.4	149.8	145.6, ^d 154.6 ^b	0.93
3	0.31	0.245	0.393, 0.376, 0.368				
<i>S</i> -7				152.8	144.2 ^d	157.5 ^b	0.93
<i>R</i> -8				139.7	137.6	149.5, ^a 137.6 ^e	
4	0.32	0.245	0.434, 0.339				0.93
<i>S</i> -8				141.5	149.1 ^a	131.5 ^e	

^a Phenyl-in. ^b Anisyl-in. ^c Tollyl-in. ^d Cyclopentyl-in. ^e *n*-Hexyl-in.

C=O dihedral angle calculated for each complex together with the experimental $a_{\beta-H}$ value ($\theta = \text{H}-\text{C}-\text{C}=\text{O} - 90^\circ$). The correlation between the experimental ($a_{\beta-H}$) and calculated data ($\cos^2 \theta$) appears to be only qualitative because the H–C–C=O angle for the *tert*-butyl-in complex is between those for the others-in complexes, but the $a_{\beta-H}$ value for the *tert*-butyl-in complex is either the largest or the smallest of the group for most of the studied compounds (see Table 3). However, $a_{\beta-H}$ appears to correlate with the distance (*d*) or with 1/*d*, having *r* values similar to those for a_N ($0.84 < r < 0.98$). This correlation with *d* possibly indicates that bulkiness of the substituent on N has more importance than the conformation of the nitroxide radical in this system. Multilinear regression of $a_{\beta-H}$ against $\cos^2 \theta$ and *d* gave better correlation coefficients ($0.93 < r < 0.99$). Since no experimental difference for the $a_{\beta-H}$ values corresponding to different diastereoisomers was observed, values for others-in complexes were assigned in the same numerical order as distances. In most cases, several hypotheses are plausible, and each was checked. Best correlation coefficients are gathered in Table 3.

The behavior of 1, 2, 5, and 6, having two aromatic rings attached on the α -C, is as described.³⁰ $a_{\beta-H}$ is greater in *tert*-butyl-in complexes because (a) the dihedral angle H–C–C=O tends to decrease with respect to the isolated guest and (b) the volume of the group directly attached to the nitrogen increases (from *tert*-butyl to the *tert*-butyl/ β -CD complex). On the other hand, substitution by more bulky groups attached on the methyl group of *N*-arylmethyl *N*-*tert*-butyl nitroxides^{27–30} makes $a_{\beta-H}$

smaller, and the differences between their values for other-in (inclusion by any group other than *tert*-butyl) complexes may be due to changes on the dihedral angle, especially in diastereomeric pairs. The larger $a_{\beta-H}$ values for the other-in complexes for 7 and 8, in spite of having similar dihedral angles, may be due to the lower electronegativity of the cyclopentyl ring and *n*-hexyl chain *vs* aromatic rings. The experimental $a_{\beta-H}$ values for free 3 and 4 and for their *tert*-butyl-in complexes do not totally agree with the values calculated for 7 and 8. We should recall that 1 and 2 have two aromatic substituents while 3 and 4 have only one. The ability of aromatic rings to form hydrogen bonds is well-known.^{31–34} The solvation of 1 and 2 is probably very different from that of 3 and 4, which may produce some structural and conformational changes that would modify the H–C–C=O torsional angle.

The greatest variation in the calculated H–C–C=O angles corresponds to the *tert*-butyl-in complexes, but they were already assigned by the a_N value. Theoretical diastereomeric differences for the dihedral angles have been found for all modeled inclusion complexes but were experimentally detected only for 2 and 3. Surprisingly, 1 does not show diastereomeric complexes in the EPR–ENDOR spectrum, but related compounds like 2 and 3 do, and the *N*-diphenylmethyl *N*-*tert*-butyl nitroxide, 11,

(31) Toda, F.; Tanaka, K.; Stein, Z.; Goldberg, I. *J. Chem. Soc., Perkin Trans. 2*, **1993**, 2359.

(32) Atwood, J. L.; Hamada, F.; Robinsin, K. D.; Orr, G. W.; Vincent, R. L. *Nature* **1991**, *349*, 683.

(33) Al-Juaid, S. S.; Al-Nasr, A. K. A.; Eaborn, C.; Hitchcock, P. B. *J. Chem. Soc., Chem. Commun.* **1991**, 1482.

(34) Karlström, G.; Linse, P.; Wallqvist, A.; Jönsson, B. *J. Am. Chem. Soc.* **1983**, *105*, 3777.

(30) Kotake, Y.; Janzen, E. G. *J. Am. Chem. Soc.* **1989**, *111*, 2066.

also shows two different phenyl-in complexes³⁵ derived from inclusion of the diastereotopic phenyl rings.

Conclusions

Molecular mechanics calculations give good correlations between experimental hyperfine splittings and calculated complex geometries not only within totally different molecules but also when the differences in the complexes are subtle as a consequence of being produced by the complexation of enantiomeric forms.¹³ However,

there are some limitations inherent in the method: modeling of the nitroxide group by a carbonyl and not taking into account the effect of the solvent. Special care should be taken when selecting the molecules to model and analyzing the final geometries and interactions.

Acknowledgment. The Comissionat per Universitats i Recerca de la Generalitat de Catalunya is acknowledged for a fellowship to one of us (X.S.-R.). Financial support was received from CICYT (project PB92-0611).

(35) Janzen, E. G.; Kotake, Y. *J. Am. Chem. Soc.* **1988**, *110*, 7912.